

# A 110-GHz Push-Push Balanced Colpitts Oscillator Using 0.15- $\mu\text{m}$ GaN HEMT Technology

**Abstract**— The paper presents a push-push sub-THz balanced Colpitts oscillator using 0.15- $\mu\text{m}$  GaN HEMTs technology. A balanced Colpitts topology is proposed to achieve a very high frequency while also with high output power. The CPW transistor was employed to allow using the transmission line (TL) source capacitance for improved negative resistance, and an in-house source-floating transistor model is built for design optimization. Also, the layout is in Grounded-CPW (GCPW) configuration with an optimized low-loss TL structure. The measured results show that the GaN oscillator can reach a peak output power of -2.1 dBm with a tuning range from 107.9~109.5 GHz, and the phase noise is -110.8 dBc/Hz at a 10 MHz offset.

**Keywords**— Sub-THz, oscillator, Push-push, GaN HEMT, small signal model.

## I. INTRODUCTION

Wireless communication and radar sensing and imaging using sub-THz/THz technologies have recently been an appealing research topic and industry application. One issue is the so-called “THz gap” because the technology for the signal generation with sufficient output power is still very challenging in this frequency range. The conventional approach uses relatively bulky optical devices for THz signal generation [3]. With the advantages of large breakdown voltage and high saturation velocity, the GaN-based devices are promising for such applications. GaN MMIC oscillators operating in the range of mm-wave and sub-THz have been reported, and good results were obtained even up to 180 GHz using 60-nm GaN HEMT technology [1]-[2].

This paper reports a push-push balanced Colpitts oscillator using 0.15- $\mu\text{m}$  GaN HEMT. Using the Colpitts topology with the feedback capacitance realized by the transistor parasitic capacitance, the proposed oscillator can reach a very high operating frequency under a relatively low power consumption. Unlike the typically used source-grounded transistor, three-terminal transistors are employed and an in-house three-terminal small-signal model is built to design the source capacitance in the Colpitts topology. Also, the grounded coplanar waveguide (GCPW) structure utilizing the backside metal and Through-wafer-vias (TWV) is optimized by full-wave EM simulation to achieve low-loss transmission for sub-THz operation. The proposed oscillator realized an output frequency of 109.5 GHz and an output power of -2.1 dBm. To the best knowledge of the authors, the proposed GaN oscillator reaches the highest oscillation frequency compared with prior reported works using the GaN HEMT technologies with the same gate length.

## II. CIRCUIT TOPOLOGY AND DESIGN CONSIDERATIONS

A push-push balanced Colpitts oscillator with the 2<sup>nd</sup> harmonic output is proposed as shown in Fig. 1(a). Fig. 1(b)

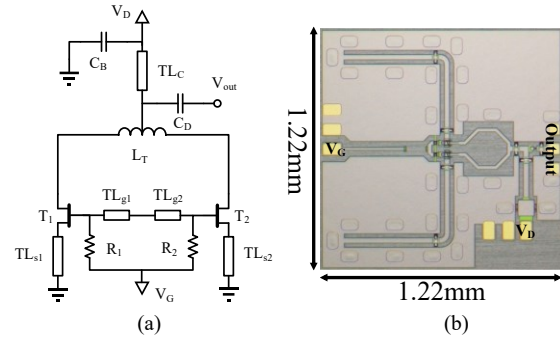


Fig. 1. Schematic(a) and chip photo(b) of the proposed oscillator.

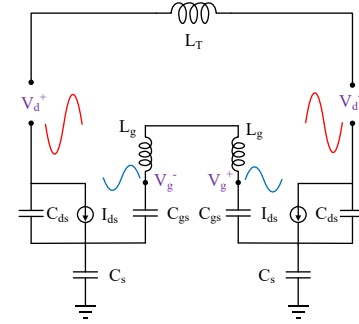


Fig. 2. Small-signal equivalent circuit model of the oscillator (excluding 2<sup>nd</sup> harmonic output).

shows the MMIC micrograph, fabricated by WIN Semiconductor 0.15- $\mu\text{m}$  GaN HEMT technology.

### A. Push-push Balanced Colpitts Topology

The balanced Colpitts topology is employed in this design. As shown in Fig. 1(a),  $TL_{g1}$  and  $TL_{g2}$  are the transmission lines that connect balanced transistors.  $TL_{s1}$  and  $TL_{s2}$  provide the DC path to the ground as well as the required capacitance  $C_s$  at the fundamental frequency ( $f_0$ ). In addition,  $L_T$  is the resonating inductor for the LC tank. The equivalent small-signal model of the resonating core at the fundamental tone is shown in Fig. 2. The drain nodes of the two transistors feature anti-phase oscillation signals at  $f_0$ , enabling the in-phase combination of 2<sup>nd</sup> harmonic ( $2f_0$ ) at the center node of the resonating tank inductor  $L_T$ . It should be emphasized that the capacitive feedback path of the Colpitts oscillator is formed by the parasitic capacitance  $C_{ds}$  of the GaN transistor as well as the equivalent source capacitance  $C_s$  realized by  $TL_{s1}$  and  $TL_{s2}$ . A properly designed source capacitance can enhance the negative resistance under low power consumption. By using the relatively small parasitic  $C_{ds}$  directly for another feedback capacitor, this topology can achieve high-frequency and low-power operation simultaneously.

### B. Three-terminal GaN Transistor Modeling

Considering the transistor breakdown voltage exceeding 120 V and the maximum current density of  $\sim 1\text{A/mm}$ , a transistor size of  $2\times 30\ \mu\text{m}$  is selected to meet the desired operating frequency and output power. The transistors are fabricated on 100- $\mu\text{m}$  GaN/SiC wafer, and the top metal layers can be connected to the backside metal using the Through-wafer-vias (TWV) in the size of  $60\ \mu\text{m} \times 30\ \mu\text{m}$ . Note that the typical device provided by the foundry is with the source connected to the backside ground through the TWVs, and the corresponding device model only has two terminals. This becomes an issue since the Colpitts topology in the proposed design needs to have the source connected to a capacitor instead of connecting to ground directly.

The source-floating transistor with the backside via removed is employed to solve this problem, and a customized small-signal transistor model is established and validated [5] for design optimization. Fig. 3 shows the schematic of the small-signal model of the GaN HEMT. The initial value of each passive component in the model is extracted by the pinch-off Cold-FET method. The Levenberg-Marquardt algorithm is used for each parameter iteration for fast convergence. Table 1 lists all the parameters in the model for a  $2\times 30\ \mu\text{m}$  GaN ( $V_G = -1.5\ \text{V}$  and  $V_D = 25\ \text{V}$ ). Fig. 4 shows validation of the established 3-terminal model by comparing the S-parameters with the foundry provided 2-port model. Based on the established 3-terminal model, the parasitic inductance due to the TWV can be removed, which can be used for design and optimization of  $C_S$  in the proposed push-push Colpitts oscillator.

### C. Oscillator Design and Optimization

Generation of negative resistance  $R_{\text{neg}}$  is probably the most important step in oscillator design. Connecting a source capacitor in an FET transistor can increase the unstable region, and enhance the negative resistance. As illustrated in Fig. 1, the transmission lines  $TL_s$  are designed for obtaining capacitive element at the source of the transistor and also for DC bias. Fig. 5(a) shows the simulated  $R_{\text{neg}}$  versus the length of  $TL_s$  (exceeding a quarter wavelength at  $f_0$ ), together with the associated equivalent capacitance of  $TL_s$ . The figure indicates that  $R_{\text{neg}}$  can be increased with shorter  $TL_s$ , showing a raised possible oscillation frequency. In the final design, the length of  $TL_s$  is designed as  $\sim 1000\ \mu\text{m}$  ( $C_s \sim 18.5\ \text{fF}$ ) with a simulated  $R_{\text{neg}}$  of  $\sim -40\ \Omega$ , which is sufficient for compensating the loss and meeting starting condition. An octagon-like tank inductor  $L_T$  is designed for saving the chip area which consumes **0.069**  $\text{mm}^2$ . At the center node of  $L_T$ , signal from the balanced branch is combined, where out-of-phase  $f_0$  is canceled by each other and in-phase  $2^{\text{nd}}$  harmonic frequency ( $2f_0$ ) is combined. A quarter wavelength transmission line at  $2f_0$  with bypass capacitor is used for providing the drain bias voltage, and DC block  $C_D$  at  $2f_0$  is used in the output path. The LC circuit also features high-pass filter which further suppresses the  $f_0$  leakage by **8 dB**. Optimization of the transmission line structure is another critical issue for the circuit operating at such high frequencies. The SiC substrate in the GaN technology is 100-the relative dielectric constant of 9.7, which can be referred to as a “electrically thick” substrate at the desired operating

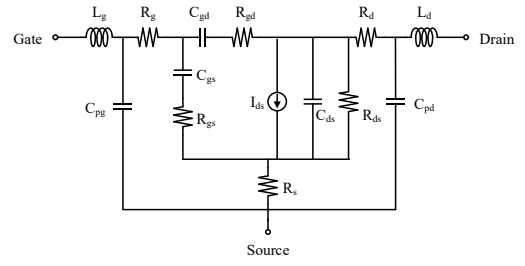


Fig. 3. Small-signal equivalent circuit model of the GaN HEMT.

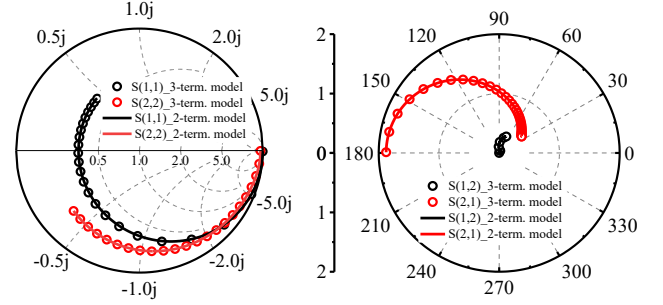


Fig. 4. Comparison of S-parameters between the foundry-provided 2-terminal and the customized 3-terminal model.

Table 1. Parameters of the Small-signal Model

$L_s$ (pH)	$L_d$ (pH)	$L_g$ (pH)	$R_s$ ( $\Omega$ )	$R_g$ ( $\Omega$ )	$R_d$ ( $\Omega$ )	$R_{gs}$ ( $\Omega$ )	$R_{ds}$ ( $\Omega$ )
22.06	23.65	35.13	9.01	7.15	11.73	3.38	4450
$R_{gd}$ ( $\Omega$ )	$C_{pg}$ (fF)	$C_{pd}$ (fF)	$C_{gd}$ (fF)	$C_{gs}$ (fF)	$C_{ds}$ (fF)	$g_m$ (mS)	
23	13.74	13.35	4.44	114.7	14.39	22.94	

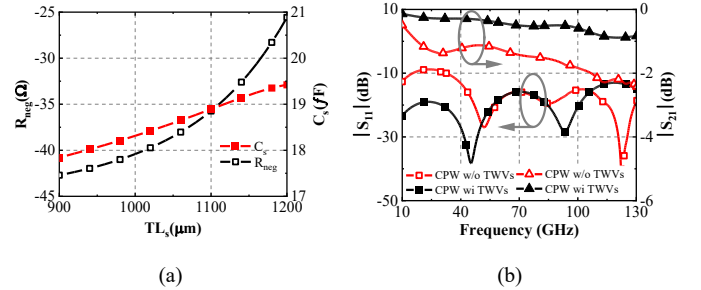


Fig. 5. (a) Negative resistance of the balanced core and the equivalent capacitance  $C_s$  of  $TL_s$  versus the length of  $TL_s$  (b) Return loss and insertion loss of the two CPWs with and without TWVs.

frequency [6]. Implementing the microstrip line would introduce high radiation loss. Therefore, the CPW structure is used for the proposed design. Fig. 6 compares the reflection coefficient and the insertion loss of the CPWs with and without the TWVs, at the lengths of  $2\lambda$  at 110 GHz, respectively. With below -10 dB reflection loss designed at the input and output, the GCPW with TWVs exhibits 1.36 dB smaller loss than that of the CPW with floating ground at 110 GHz. Note that the spacing between TWVs is designed based on both design rules and analytical model from [8], and the airbridge using layer metal 2 is utilized to balance the electric potential in the discontinuity.

Table 2. Performance Comparison with Prior Sub-THz GaN Oscillators

Refs	GaN HEMT Tech.	Topology	Frequency (GHz)	$f_0/f_T$ (GHz)	$f_0/f_{max}$ (GHz)	$P_{out}$ (dBm)	$P_{DC}$ (mW)	PN (dBc/Hz)
[1]	60 nm	Push-push	180.6*	0.47	0.36	9.3	920	-88.2@10MHz
[2]	60 nm	Common-gate Colpitts	84	0.44	0.34	-0.67	340	-120@10MHz
[4]	100 nm	Single-end	89.2	1.11	0.44	10.2	650	-90.2@1MHz
This work	150 nm	Push-push	109.5*	1.71	0.4	-2.1	295.5	-77.4@1MHz -110.8@10MHz

\*: 2<sup>nd</sup> harmonic

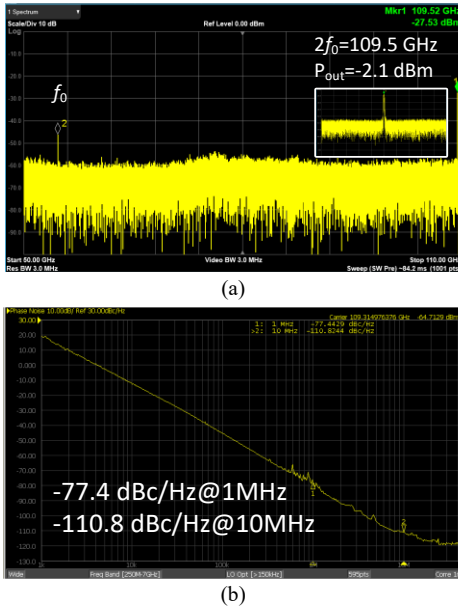


Fig. 6. Measure spectrum(a) and phase noise(b) of the proposed oscillator.

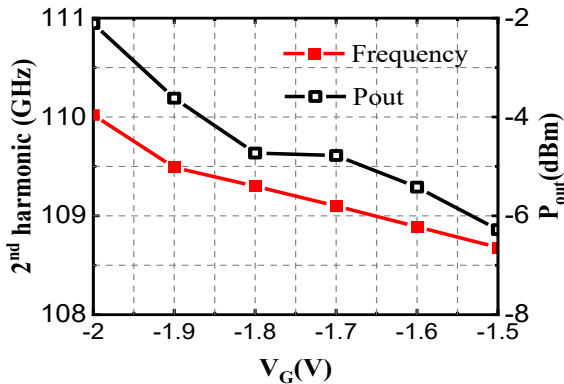


Fig. 7. Measured oscillation frequency and output power as versus the gate bias voltage.

### III. MEASURED RESULTS AND DISCUSSION

The chip was measured on-wafer up to 110 GHz using the spectrum analyzer (Keysight N9041B UXA) for oscillation frequency of the fundamental and the 2<sup>nd</sup> harmonic, and the signal source analyzer (Keysight E5052A) with downconverter (Keysight E5053A) and 110-GHz harmonic mixers (Keysight 11970W) was used for phase noise measurement. Under a

power consumption of 295.5 mW, the measured output signal frequency is 109.5 GHz with a power level of -2.1 dBm after calibration of cable loss, as shown in Fig. 6(a). Fig. 6(b) shows measured phase noise, which is -110.8 dBc/Hz at a 10-MHz offset. Fig. 7 shows the frequency tuning range and output power of the 2<sup>nd</sup> harmonic frequency as  $V_G$  varies from -1.5 to -2 V. To the best of the authors' knowledge, this work reports the highest oscillation frequency based on a 0.15- $\mu$ m GaN HEMT technology. Table 2 also compares the reported sub-THz oscillators using GaN HEMTs with different gate lengths. This work exhibits comparable oscillation frequency with high  $f_0/f_T$  and  $f_0/f_{max}$  ratio.

### IV. CONCLUSION

This paper presented a sub-THz push-push balanced Colpitts oscillator up to 110 GHz based on 0.15- $\mu$ m GaN HEMT technology. The in-house 3-terminal model was built for designing the source capacitor for negative resistance enhancement. The GCPW transmission line configuration was adopted to minimize signal loss. Also, by using the relatively small parasitic capacitor for the feedback path, the oscillator can achieve high frequency and low power operation simultaneously. The measured results demonstrated the highest operating frequency compared with other reported works using GaN HEMT with the same gate length, which is suitable for the emerging applications of millimeter-wave radar imaging and sensing systems.

### REFERENCES

- [1] Kim, D. and S. Jeon, "W- and G-Band GaN voltage-controlled oscillators with high output power and high efficiency," in *IEEE Trans. Microwave Theory Tech.*, vol. 69, no. 8, p. 3908-3916, Aug. 2021.
- [2] Thi Do, T.N., Y. Yan, and D. Kuylenstierna, "A low phase noise W-band MMIC GaN HEMT oscillator", in *Proc. IEEE Asia-Pacific Microwave Conf.*, 2020, p. 113-115.
- [3] Saeedkia, D. and S. Safavi-Naeini, "Terahertz photonics: optoelectronic techniques for generation and detection of terahertz waves," *Journal of Lightwave Technol.*, vol. 26, no. 15, p. 2409-2423, Aug. 2008.
- [4] Weber, R., et al., "A 92 GHz GaN HEMT voltage-controlled oscillator MMIC", in *Proc. IEEE MTT-S Int. Microwave Symp.*, 2014, p. 1-4.
- [5] Emekar, S., et al., "Modified angelov model for an exploratory GaN-HEMT technology with short few-fingered gates," in *Proc. Int. Conf. Simulation of Semicond. Processes and Devices*, 2017, p. 117-120.
- [6] Garg, R., Bhartia, P., Bahl, I. J., Ittipiboon, A., *Microstrip antenna design handbook*. New York, USA: Artech house, 2001.